

# Studying QCD factorizations in exclusive $\gamma^* \gamma^* \rightarrow \rho_L^0 \rho_L^0$

S. Wallon<sup>1†</sup>, B. Pire<sup>2</sup>, M. Segond<sup>1</sup>, L. Szymanowski<sup>3</sup>

<sup>1</sup> LPT, Université Paris-Sud, CNRS, Orsay, France,

<sup>2</sup> CPHT, École Polytechnique, CNRS, Palaiseau, France,

<sup>3</sup> IFPA, Université de Liège, Belgium and SINS, Warsaw, Poland

## Abstract

The exclusive process  $e^+ e^- \rightarrow e^+ e^- \rho_L^0 \rho_L^0$  allows to study various dynamics and factorization properties of perturbative QCD. At moderate energy, we demonstrate how collinear QCD factorization emerges, involving generalized distribution amplitudes (GDA) and transition distribution amplitudes (TDA). At higher energies, in the Regge limit of QCD, we show that it offers a promising probe of the BFKL resummation effects to be studied at the International Linear Collider (ILC).

## 1 Introduction: Exclusive processes at high energy QCD

### 1.1 Motivation

Since a decade, there has been much progress in experimental and theoretical understanding of hard exclusive processes, including Deeply Virtual Compton Scattering (involving Generalized Parton Distributions) and  $\gamma\gamma$  scattering in fixed target  $e^\pm p$  (HERMES, JLab, ...) experiments and at colliders, such as  $e^\pm p$  (H1, ZEUS) or  $e^+ e^-$  (LEP, Belle, BaBar, BEPC). Meanwhile, the hard Pomeron [1] concept has been developed and tested at inclusive (total cross-section), semi-inclusive (diffraction, forward jets, ...) and exclusive (meson production) level, for colliders at very large energy:  $e^\pm p$  (HERA),  $p\bar{p}$  (Tevatron) and  $e^+ e^-$  (LEP, ILC). Here we focus on

$$\gamma^* \gamma^* \rightarrow \rho_L^0 \rho_L^0 \quad (1)$$

with both  $\gamma^*$  hard, through  $e^+ e^- \rightarrow e^+ e^- \rho_L^0 \rho_L^0$  with double tagged outgoing leptons (Fig.1). It is a beautiful theoretical laboratory for investigating different *dynamics* (collinear, multiregge) and *factorization* properties of high energy QCD: it allows a perturbative study of GPD-like objects at moderate  $s$  and of the hard Pomeron at asymptotic  $s$ .

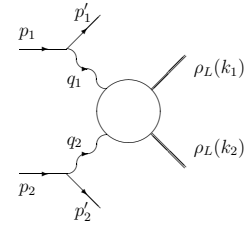


Figure 1: Amplitude for  $e^+ e^- \rightarrow e^+ e^- \rho_L^0 \rho_L^0$ .

### 1.2 From DIS to GDA and TDA in collinear factorization

Deep Inelastic Scattering, as an inclusive process, gives access to the forward amplitude through the optical theorem. Structure functions can be written as convolution of (hard) Coefficient Functions with (soft) Parton Distributions. Deeply Virtual Compton Scattering and meson electroproduction on a hadron  $\gamma^* h \rightarrow \gamma h, h' h$ , as exclusive processes, give access to the full amplitude, which is a convolution, for  $-t \ll s$ , of a (hard) CF with a (soft) Generalized Parton Distribution [2,3]. Extensions were made from GPDs. First [2,4], the crossed process  $\gamma^* \gamma \rightarrow h h'$  can be factorized, for  $s \ll -t$ , as a convolution of a (hard) CF with a (soft) Generalized Distribution

<sup>†</sup> talk presented at EDS07

Amplitude describing the correlator between two quark fields and a two hadron state. Second [5], starting from meson electroproduction and performing  $t \leftrightarrow u$  crossing, and then allowing the initial and the final hadron to differ, we write the amplitude for the process  $\gamma^* h \rightarrow h'' h'$  as a convolution of a (hard) CF with a (soft) Transition Distribution Amplitude describing the  $h \rightarrow h'$  transition and with a (soft) Distribution Amplitude (describing  $q\bar{q}h''$  vertex).

We will rely on collinear factorization for our process (1) at each  $q\bar{q}\rho$  vertex only. At high  $Q_i^2$ , each of the two quarks making the  $\rho$  mesons are almost collinear, flying in the light cone directions  $p_1$  and  $p_2$  (used as Sudakov vectors), and their momentum read  $\ell_i \sim z_i k_i$  and  $\bar{\ell}_i \sim \bar{z}_i k_i$ . The amplitude  $M$  is factorized as a convolution of a hard part  $M_H$  with two  $\rho_L^0$  DAs (see Fig.2), defined as matrix elements of non local quarks fields correlator on the light cone<sup>1 2</sup>

$$\langle \rho_L^0(k) | \bar{q}(x) \gamma^\mu q(0) | 0 \rangle = \frac{f_\rho}{\sqrt{2}} k^\mu \int_0^1 dz e^{iz(kx)} \phi(z), \quad \text{for } q = u, d.$$

## 2 Computation at fixed $W^2$

### 2.1 Direct calculation

We compute [6] the amplitude  $M$  following the Brodsky, Lepage approach [7]. At Born order (quark exchange) and in the forward case for simplicity, the amplitude  $M$  reads<sup>3</sup>,

$$M = T^{\mu\nu} \epsilon_\mu(q_1) \epsilon_\nu(q_2), \quad T^{\mu\nu} = \frac{1}{2} g_T^{\mu\nu} T^{\alpha\beta} g_{T\alpha\beta} + \left( p_1^\mu + \frac{Q_1^2}{s} p_2^\mu \right) \left( p_2^\nu + \frac{Q_2^2}{s} p_1^\nu \right) \frac{4}{s^2} T^{\alpha\beta} p_{2\alpha} p_{1\beta}.$$

In the case of longitudinally polarized photons, their polarization vectors read, with  $s \equiv 2 p_1 \cdot p_2$ ,

$$\epsilon_\parallel(q_1) = \frac{1}{Q_1} q_1 + \frac{2Q_1}{s} p_2 \quad \text{and} \quad \epsilon_\parallel(q_2) = \frac{1}{Q_2} q_2 + \frac{2Q_2}{s} p_1. \quad (2)$$

Due to QED gauge invariance, the first terms in RHS of (2) do not contribute. In the forward case discussed here, the number of diagrams then reduces to 4, as illustrated in Fig.3. They result into

$$T^{\alpha\beta} p_{2\alpha} p_{1\beta} = - \frac{s^2 f_\rho^2 C_F e^2 g^2 (Q_u^2 + Q_d^2)}{8 N_c Q_1^2 Q_2^2} \int_0^1 dz_1 dz_2 \phi(z_1) \phi(z_2) \times \left\{ \frac{(1 - \frac{Q_1^2}{s})(1 - \frac{Q_2^2}{s})}{(z_1 + \bar{z}_1 \frac{Q_2^2}{s})(z_2 + \bar{z}_2 \frac{Q_1^2}{s})} + \frac{(1 - \frac{Q_1^2}{s})(1 - \frac{Q_2^2}{s})}{(\bar{z}_1 + z_1 \frac{Q_2^2}{s})(\bar{z}_2 + z_2 \frac{Q_1^2}{s})} + \frac{1}{z_2 \bar{z}_1} + \frac{1}{z_1 \bar{z}_2} \right\}. \quad (3)$$

<sup>1</sup> We limit ourselves to longitudinally polarized mesons to avoid potential end-point singularities.

<sup>2</sup>  $\phi(z) = 6z(1-z)(1 + \sum_{n=1}^\infty a_{2n} C_{2n}^{3/2}(2z-1))$ .

<sup>3</sup>  $g_T^{\mu\nu} = g^{\mu\nu} - \frac{p_1^\mu p_2^\nu + p_2^\mu p_1^\nu}{p_1 \cdot p_2}$ .

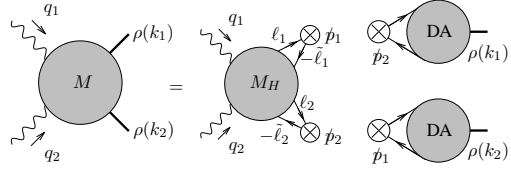


Figure 2:  $\gamma^*(Q_1) \gamma^*(Q_2) \rightarrow \rho_L^0(k_1) \rho_L^0(k_2)$  with collinear factorization in  $q\bar{q}\rho$  vertices.

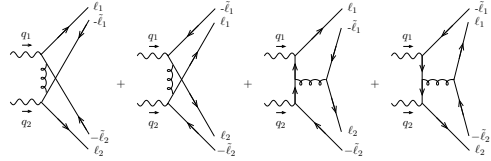


Figure 3: Diagrams contributing to  $M_H$  for  $\gamma_L^*$ .

For transversally polarized photons, no simplification occurs and the 12 diagrams give

$$\begin{aligned}
T^{\alpha\beta} g_{T\alpha\beta} = & -\frac{e^2(Q_u^2 + Q_d^2) g^2 C_F f_\rho^2}{4 N_c s} \int_0^1 dz_1 dz_2 \phi(z_1) \phi(z_2) \left\{ 2 \left( 1 - \frac{Q_2^2}{s} \right) \left( 1 - \frac{Q_1^2}{s} \right) \right. \\
& \times \left[ \frac{1}{(z_2 + \bar{z}_2 \frac{Q_1^2}{s})^2 (z_1 + \bar{z}_1 \frac{Q_2^2}{s})^2} + \frac{1}{(\bar{z}_2 + z_2 \frac{Q_1^2}{s})^2 (\bar{z}_1 + z_1 \frac{Q_2^2}{s})^2} \right] + \left( \frac{1}{\bar{z}_2 z_1} - \frac{1}{\bar{z}_1 z_2} \right) \\
& \times \left[ \frac{1}{1 - \frac{Q_2^2}{s}} \left( \frac{1}{\bar{z}_2 + z_2 \frac{Q_1^2}{s}} - \frac{1}{z_2 + \bar{z}_2 \frac{Q_1^2}{s}} \right) - \frac{1}{1 - \frac{Q_1^2}{s}} \left( \frac{1}{\bar{z}_1 + z_1 \frac{Q_2^2}{s}} - \frac{1}{z_1 + \bar{z}_1 \frac{Q_2^2}{s}} \right) \right] \left. \right\}. \quad (4)
\end{aligned}$$

The  $z_i$  integrations have no end-point singularity ( $Q_i^2$  are non-zero and DAs vanishes at  $z_i = 0$ ).

## 2.2 Interpretation in terms of QCD Factorization

### 2.2.1 GDA for transverse photon in the limit $\Lambda_{QCD}^2 \ll W^2 \ll \text{Max}(Q_1^2, Q_2^2)$

When  $W^2$  is smaller than the highest photon virtuality, the direct calculation (4) simplifies in<sup>4</sup>

$$T^{\alpha\beta} g_{T\alpha\beta} \approx \frac{C}{W^2} \int_0^1 dz_1 dz_2 \left( \frac{1}{\bar{z}_1 + z_1 \frac{Q_2^2}{s}} - \frac{1}{z_1 + \bar{z}_1 \frac{Q_2^2}{s}} \right) \left( \frac{1}{\bar{z}_2 z_1} - \frac{1}{\bar{z}_1 z_2} \right) \phi(z_1) \phi(z_2)$$

showing that the hard amplitude  $M_H$  can be factorized as a convolution between a hard coefficient function  $T_H$  and a  $GDA_H$ , itself *perturbatively* computable (Fig.4), extending the results of [8]. This is proven at Born order by computing perturbatively the GDA from its definition

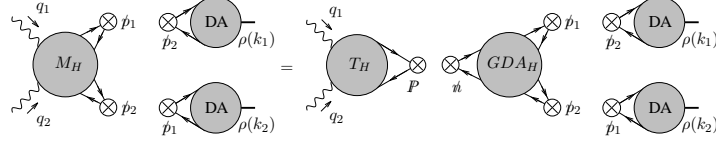
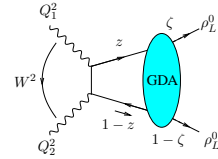


Figure 4: Factorisation of the amplitude in terms of a GDA.

$$\begin{aligned}
& \langle \rho_L^0(k_1) \rho_L^0(k_2) | \bar{q}(-\alpha n/2) \not{n} \exp \left[ ig \int_{-\frac{\alpha}{2}}^{\frac{\alpha}{2}} dy n_\nu A^\nu(y) \right] q(\alpha n/2) | 0 \rangle \\
& = \int_0^1 dz e^{-i(2z-1)\alpha(nP)/2} \Phi \rho_L^0 \rho_L^0(z, \zeta, W^2) \quad (\text{for } Q_1 > Q_2, P \sim p_1 \text{ and } n \sim p_2)
\end{aligned}$$

with the kinematics fixed according to Fig.5.  $W^2$  being hard, the GDA can be factorized into Hard part  $\otimes$  DA DA (see Fig.6), as



$$\Phi^{\rho_L \rho_L}(z, \zeta \approx 1, W^2) = -\frac{f_\rho^2 g^2 C_F}{2 N_c W^2} \int_0^1 dz_2 \phi(z) \phi(z_2) \left[ \frac{1}{z \bar{z}_2} - \frac{1}{\bar{z} z_2} \right]. \quad \text{Figure 5: GDA Kinematics.}$$

<sup>4</sup>In this example  $\frac{W^2}{Q_1^2} = \frac{s}{Q_1^2} \left( 1 - \frac{Q_1^2}{s} \right) \left( 1 - \frac{Q_2^2}{s} \right) \approx 1 - \frac{Q_1^2}{s} \ll 1$ ; we denote  $C = \frac{e^2(Q_u^2 + Q_d^2) g^2 C_F f_\rho^2}{4 N_c}$

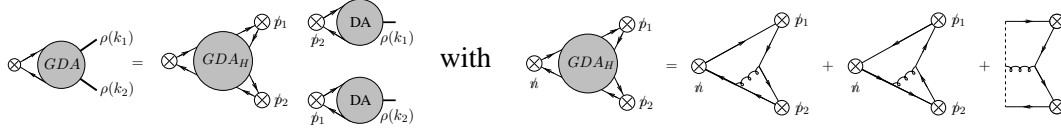


Figure 6: Perturbative GDA factorization.

In forward kinematics, the QCD Wilson line (last term in Fig.6) vanishes. The Born order hard part is (see Fig.7)

$$T_H(z) = -4e^2 N_c Q_q^2 \left( \frac{1}{\bar{z} + z \frac{Q_2^2}{s}} - \frac{1}{z + \bar{z} \frac{Q_2^2}{s}} \right).$$

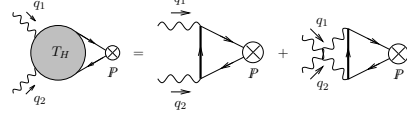


Figure 7: Hard part  $T_H$  at lowest order.

### 2.2.2 TDA for longitudinal photon in the limit $Q_1^2 \gg Q_2^2$ (or $Q_1^2 \ll Q_2^2$ )

The amplitude  $M = T^{\alpha\beta} p_{2\alpha} p_{1\beta}$  (3) can be interpreted in this limit as a convolution  $M = TDA \otimes CF \otimes DA$ , according to

$$T^{\alpha\beta} p_{2\alpha} p_{1\beta} = -i \frac{C}{2} \int_{-1}^1 dx \int_0^1 dz_1 \left[ \frac{1}{\bar{z}_1(x-\xi)} + \frac{1}{z_1(x+\xi)} \right] \phi(z_1) \times N_c \left[ \Theta(1 \geq x \geq \xi) \phi\left(\frac{x-\xi}{1-\xi}\right) - \Theta(-\xi \geq x \geq -1) \phi\left(\frac{1+x}{1-\xi}\right) \right],$$

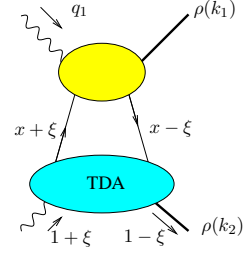


Figure 8: TDA kinematics.

the TDA being defined through the usual GPD kinematics (see Fig.8), with  $n_1 = (1+\xi)p_1$  and  $n_2 = \frac{p_2}{1+\xi}$ , defining  $x, \xi$  as momentum fraction along  $n_2$ . This factorisation (see Fig.9a) is proven at Born order by computing perturbatively the TDA  $\gamma^* \rightarrow \rho_L^0$  defined as

$$\int \frac{dz^-}{2\pi s} e^{ix(n_2 \cdot z)} \langle \rho_L^0(k_2) | \bar{q}(-z/2) n_1^\nu \exp\{-ieQ_q \int_{z/2}^{-z/2} dy_\mu A^\mu(y)\} q(z/2) | \gamma^*(q_2) \rangle$$

$$= \frac{e Q_q f_\rho}{n_2^+} \frac{1}{Q_2^2} \epsilon_\nu(q_2) \left( (1+\xi)n_2^\nu + \frac{Q_2^2}{s(1+\xi)} n_1^\nu \right) T(x, \xi, t_{min}),$$

where the QED Wilson line is explicitly indicated (QCD Wilson line gives no contribution). Since  $Q_2^2$  hard, the TDA can be factorized (see Fig.9b) as

$$T(x, \xi, t_{min}) \equiv N_c \left[ \Theta(1 \geq x \geq \xi) \phi\left(\frac{x-\xi}{1-\xi}\right) - \Theta(-\xi \geq x \geq -1) \phi\left(\frac{1+x}{1-\xi}\right) \right].$$

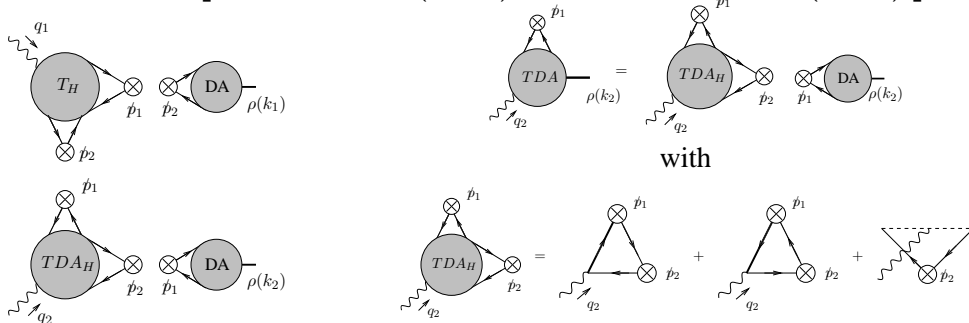


Figure 9: a: Factorization of the amplitude in terms of a TDA. b: Perturbative TDA factorization.

The Hard term reads, at Born order (see Fig.10),

$$T_H(z_1, x) = -i f_\rho g^2 e Q_q \frac{C_F \phi(z_1)}{2 N_c Q_1^2} \epsilon^\mu(q_1) \\ \times \left( 2\xi n_{2\mu} + \frac{1}{1+\xi} n_{1\mu} \right) \left[ \frac{1}{z_1(x+\xi-i\epsilon)} + \frac{1}{\bar{z}_1(x-\xi+i\epsilon)} \right],$$

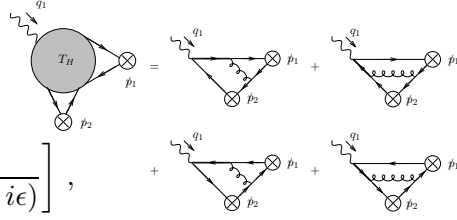


Figure 10: Hard part  $T_H$  at lowest order.

### 3 Computation at large $W^2$

The dynamics of QCD in the perturbative Regge limit [9] is governed by gluons. BFKL enhancement effects are expected to be important at large rapidity. The exclusive process (1) tests this limit [10–12], for both  $Q_i^2$  *hard* and of the *same order* (to suppress collinear dynamics à la DGLAP [13] and ERL [14]), giving access to the full non-forward Pomeron structure, in relation with saturation studies, where a full impact parameter picture is needed. Increasing  $s_{\gamma^*\gamma^*}$  for fixed values  $Q_1^2$  and  $Q_2^2$  causes transition from the linear to non-linear (saturated) regime.

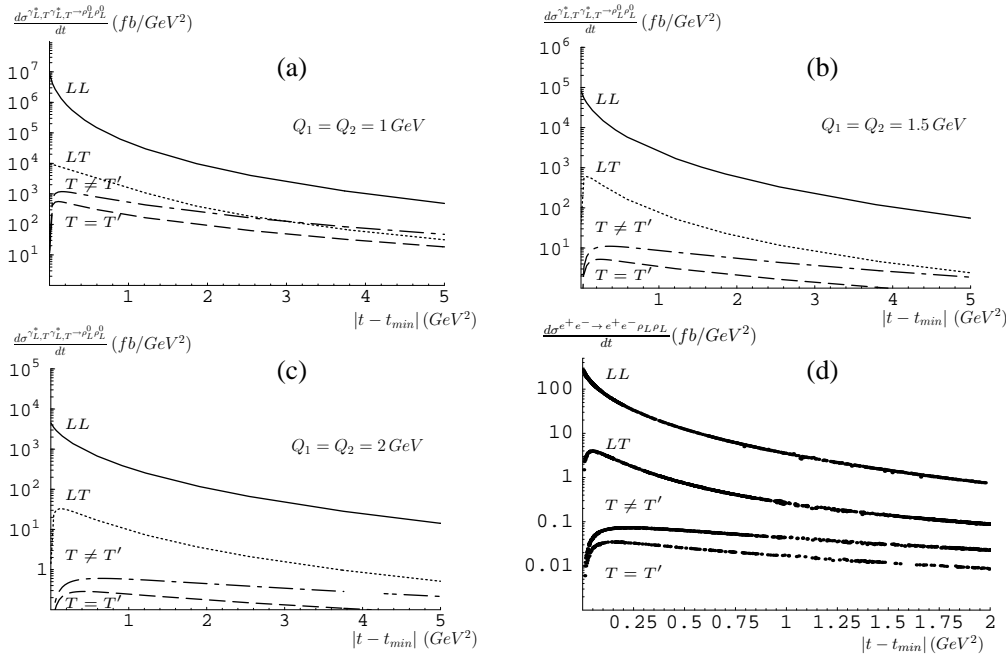


Figure 11:  $\gamma_{L,T}^* \gamma_{L,T}^* \rightarrow \rho_L^0 \rho_L^0$  (a,b,c) and  $e^+ e^- \rightarrow e^+ e^- \rho_L^0 \rho_L^0$  (d) differential cross-sections.

When  $s_{\gamma^*\gamma^*} \gg -t, Q_1^2, Q_2^2$ , we rely on the impact representation which reads, at Born order,

$$\mathcal{M} = is \int \frac{d^2 \underline{k}}{(2\pi)^4 \underline{k}^2 (\underline{r} - \underline{k})^2} \mathcal{J}^{\gamma_{L,T}^*(q_1) \rightarrow \rho_L^0(k_1)}(\underline{k}, \underline{r} - \underline{k}) \mathcal{J}^{\gamma_{L,T}^*(q_2) \rightarrow \rho_L^0(k_2)}(-\underline{k}, -\underline{r} + \underline{k})$$

where the impact factors  $\mathcal{J}^{\gamma_{L,T}^*}$  are rational functions of the transverse momenta  $(\underline{k}, \underline{r})$ . The 2-d integration is treated analytically, relying on conformal transformations in the transverse momentum plane. The integrations over momentum fractions  $z_1$  and  $z_2$  (hidden in  $\mathcal{J}$ ) are performed numerically. We use  $Q_1 Q_2$  as a scale for  $\alpha_S$ . As displayed in Fig.11a,b,c, cross-sections are strongly peaked at small  $Q^2$  and small  $t$ , and longitudinally polarized photons dominates. The

non-forward Born order cross-section for  $e^+e^- \rightarrow e^+e^- \rho_L^0 \rho_L^0$  is obtained with the help of the equivalent photon approximation. Defining  $y_i$  as the longitudinal momentum fractions of the bremsstrahlung photons, one finds that  $\sigma^{e^+e^- \rightarrow e^+e^- \rho_L \rho_L}$  gets its main contribution from the low  $y$  and  $Q^2$  region, which is the very forward region. At ILC,  $\sqrt{s_{e^+e^-}} = 500$  GeV, with  $125 \text{ fb}^{-1}$  per year. The measurement seems feasible since each detector design includes a very forward electromagnetic calorimeter for luminosity measurement, with tagging angle for outgoing leptons down to 5 mrad. In Fig.11d, we display our results within the Large Detector Concept. We obtain  $\sigma^{tot} = 34.1 \text{ fb}$  and  $4.3 \cdot 10^3$  events per year. The LL BFKL enhancement is enormous but not trustable, since it is well known that NLL BFKL is far below LL. Work to implement *resummed* LL BFKL effects [15] is in progress, with results in accordance with the NLL based one [16]. The obtained enhancement is less dramatic ( $\sim 5$ ) than with LL BFKL, but *still visible*.

## Aknowledgements

L.Sz. is supported by the Polish Grant 1 P03B 028 28. He is a Visiting Fellow of FNRS (Belgium).

## References

- [1] E.A. Kuraev, L.N. Lipatov and V.S. Fadin, Phys. Lett. B **60**, 50-52 (1975); Sov. Phys. JETP **44**, 443-451 (1976) ; Sov. Phys. JETP **45**, 199-204 (1977) ; Ya.Ya. Balitskii and L.N. Lipatov, Sov. J. Nucl. Phys. **28**, 822-829 (1978).
- [2] D. Müller, D. Robaschik, B. Geyer, F. M. Dittes, J. Hořejši, Fortsch. Phys. **42**, 101 (1994);
- [3] X. Ji, Phys. Rev. Lett. **78**, 610 (1997); Phys. Rev. D **55**, 7114 (1997); A. V. Radyushkin, Phys. Rev. D **56**, 5524 (1997); For a review, see M. Diehl, Phys. Rept. **388**, 41 (2003) and A. V. Belitsky and A. V. Radyushkin, Phys. Rept. **418**, 1 (2005).
- [4] M. Diehl, T. Gousset, B. Pire and O. Teryaev, Phys. Rev. Lett. **81**, 1782 (1998); M. Diehl, T. Gousset and B. Pire, Phys. Rev. D **62**, 073014 (2000); I. V. Anikin, B. Pire and O. V. Teryaev, Phys. Rev. D **69**, 014018 (2004).
- [5] B. Pire and L. Szymanowski, Phys. Rev. D **71**, 111501 (2005); Phys. Lett. B **622**, 83 (2005); J. P. Lansberg, B. Pire and L. Szymanowski, Phys. Rev. D **73**, 074014 (2006); Phys. Rev. D **75**, 074004 (2006) and arXiv:0709.2567 [hep-ph].
- [6] B. Pire, M. Segond, L. Szymanowski and S. Wallon, Phys. Lett. B **39**, 642-651 (2006); PoS D **IFF2006**, 034 (2006).
- [7] S. J. Brodsky and G. P. Lepage, Phys. Rev. D **24**, 1808 (1981).
- [8] M. Diehl, T. Feldmann, P. Kroll and C. Vogt, Phys. Rev. D **61**, 074029 (2000).
- [9] See talk "Perturbative QCD in the Regge limit: Prospects at ILC", arXiv:0710.0833 [hep-ph], slides: <https://indico.desy.de/conferenceDisplay.py?confId=372>
- [10] M. Segond, L. Szymanowski and S. Wallon, Eur. Phys. J. C **52**, 93 (2007) [arXiv:hep-ph/0703166].
- [11] B. Pire, L. Szymanowski and S. Wallon, Eur. Phys. J. C **44**, 545 (2005); LCWS 04, Paris, France, 19-24 Apr 2004, Published in "Paris 2004, Linear colliders, vol. 1," 335-340; Nucl. Phys. A **755** (2005) 626-629; EDS05, Blois, France, 15-20 May 2005, "Towards High Energy Frontiers", eds. M. Haguenaue et al., 373-376.
- [12] R. Enberg, B. Pire, L. Szymanowski and S. Wallon, Eur. Phys. J. C **45**, 759 (2006) [Erratum-ibid. C **51**, 1015 (2007)]; Acta Phys. Polon. B **37**, 847 (2006).
- [13] V. N. Gribov and L. N. Lipatov, Yad. Fiz. **15**, (1972) 781 [Sov. J. Nucl. Phys. **15**, 438 (1972)]; G. Altarelli and G. Parisi, Nucl. Phys. B **126**, 298 (1977); Y. L. Dokshitzer, Sov. Phys. JETP **46**, 641 (1977) [Zh. Eksp. Teor. Fiz. **73**, 1216 (1977)].
- [14] G.P. Lepage and S.J. Brodsky, Phys. Lett. B **87**, 359 (1979); A.V. Efremov and A.V. Radyushkin, Phys. Lett. B **94**, 245 (1980).
- [15] V. A. Khoze, A. D. Martin, M. G. Ryskin and W. J. Stirling, Phys. Rev. D **70**, 074013 (2004).
- [16] D. Y. Ivanov and A. Papa, Nucl. Phys. B **732**, 183 (2006) and Eur. Phys. J. C **49** 947 (2007).
- [17] slides: <https://indico.desy.de/conferenceDisplay.py?confId=372#9>